bio-protocol

Published: Mar 20, 2022

Measurement of Contractile Ring Tension Using Two-photon Laser Ablation during *Drosophila* Cellularization

Swati Sharma and Richa Rikhy*

Biology, Indian Institute of Science Education and Research, Homi Bhabha Road, Pashan, Pune, 411008, India
*For correspondence: richa@iiserpune.ac.in

Abstract

Cytokinesis occurs at the final step of cell division and leads to the separation of daughter cells. It requires assembly and constriction of the actomyosin contractile ring. The phases of assembly and constriction of the contractile ring show an increase in tension in the actomyosin complex. The measurement of tension in the contractile ring is of interest to probe the mechanics of contractile ring formation. *Drosophila* cellularization is a powerful genetic model system to study the mechanisms regulating actomyosin contractility during contractile ring constriction. Cellularization occurs in the interphase of syncytial cycle 14, where the plasma membrane extends around individual nuclei and forms complete cells with the help of a contractile ring at the bottom. The contractile ring forms at the furrow tip during the extension around individual nuclei and its assembly requires the coordinated action of cytoskeletal and plasma membrane-associated proteins. Laser ablation of the contractile ring enables the measurement of the contractility of the actomyosin network during cytokinesis. This protocol outlines the method used for estimating the contractility at the actomyosin ring during cellularization by laser ablation, in both control and mutant embryos for a Rho guanosine triphosphatase activating protein (RhoGAP) containing protein called GRAF (GTPase regulator associated with focal adhesion kinase-1). Physical cutting of the contractile ring by a two-photon laser at 800 nm leads to the displacement of the actomyosin ring edges, at a rate dependent upon the tension. This can be carried out at distinct steps of the contractile ring assembly during furrow extension in cellularization. Quantification of the extent of displacement and recoil velocity of movement of the edges at different stages of cellularization provides a quantitative measure of contractility in the system. This protocol describes the experimental procedure containing the preparation of live embryos, optimization of laser power, acquisition settings, and post-acquisition analysis of actomyosin contractility during *Drosophila* cellularization.

Keywords: Actomyosin ring constriction, Laser ablation, Contractility, Cleavage furrow, Myosin II, GRAF, Cellularization, *Drosophila*

This protocol was validated in: eLife (2021), DOI: 10.7554/eLife.63535

Background

Cell shape changes occurring during cell migration, cell division, epithelial cell formation, and gastrulation in embryogenesis require coordinated remodeling of the cytoskeleton and plasma membrane. Actomyosin contractility is regulated precisely to drive cell shape changes in embryonic development. Cortical tension is derived by a combination of cell adhesion and actomyosin contractility (Priya and Yap, 2015; Heer and Martin, 2017). Cortical tension at different stages in metazoan embryogenesis has been measured by a variety of methods, such as tension sensors using FRET, laser ablation, and atomic force microscopy (Paluch and Heisenberg, 2009; Kong *et al*., 2017).

Cytokinesis occurs at the end of cell division and is responsible for separating cytoplasmic constituents into daughter cells. The actomyosin-based contractile ring assembles at the plasma membrane in between daughter nuclei and constricts to form daughter cells. Several molecules are recruited to the contractile ring in a concerted manner during cytokinesis in animal cells, to drive changes in actomyosin contractility (Carim *et al*., 2020). *Drosophila* embryo development starts as a syncytium, with nuclear division cycles 1 to 13 occurring in a common cytoplasm without cytokinesis. Complete epithelial cells form in the interphase of nuclear cycle 14, in a process called cellularization (Foe and Alberts, 1983). The plasma membrane extends in the form of furrows around individual nuclei. The actomyosin ring assembles at the base of this furrow during extension and constricts to close off the cells (Xue and Sokac, 2016).

The actomyosin complex assembly occurs at the furrow tip in the early stages of plasma membrane invagination in cellularization. Change in the actomyosin assembly organization at the furrow tip from polygonal to circular, followed by constriction of the ring, occurs during mid and late stages of furrow extension (Xue and Sokac, 2016). The rate of actomyosin assembly and constriction depends upon a collaboration between molecules of cytoskeletal and membrane-associated machinery along with the Rho-Rho Kinase-Myosin II pathway. Increased recruitment of Rho guanosine triphosphate (RhoGTP) exchange factor Rho guanine nucleotide exchange factor 2, isoform E (RhoGEF2) leads to an increase in contractility of the actomyosin ring (Krueger *et al*., 2019).

Laser ablation has been used as a method to measure actomyosin ring contractility during *Drosophila* cellularization (He *et al*., 2016; Krueger *et al*., 2019; Sharma and Rikhy, 2021). Laser ablation at the early stages of contractile ring assembly shows displacement of the edges, thereby showing that the assembling actomyosin network is interconnected and under tension (He *et al.*, 2016). Further laser ablation has been performed at different stages of ring assembly on induction of Rho-GTP exchange factor RhoGEF2. The hexagonal phase of actomyosin assembly shows decreased contractility upon laser ablation even after the activation of RhoGEF2, as compared to ring stages (Krueger *et al*., 2019). These data suggest the presence of an inhibitor of constriction in the hexagonal phases of actomyosin assembly. Our recent studies showed that mutants of RhoGAP containing protein GRAF show increased levels of RhoGTP and Myosin II (Sharma and Rikhy, 2021). Laser ablation of the ring at early and mid-stages of *Graf* mutant embryos shows an increased displacement of the edges as compared to controls. Laser ablation can therefore be used to systematically assess the change in contractility of the network under different genetic backgrounds, to elucidate the mechanisms that regulate the onset and progression of the contractile ring during cellularization. Here, we outline the method for measuring actomyosin ring contractility during *Drosophila* cellularization, using two-photon assisted laser ablation in control and *Graf* mutant fly embryos. A physical lesion in the ring is created by the two-photon laser at 800 nm at the furrow tips in different stages of cellularization. The displacement of the edges is measured at subsequent time points, and the rate of displacement is calculated to document the recoil velocity (Liang *et al*., 2016; Krueger *et al*., 2019; Sharma and Rikhy, 2021). We outline the procedure for each of the steps of sample preparation, followed by ablation, measurement of edge movement, and recoil velocity in control embryos and hyper contractile *Graf* mutant embryos (Sharma and Rikhy, 2021).

Materials and Reagents

1. Petri plates (60 mm, Tarsons, India, catalog number: 460061)
2. Cell strainer (Corning, catalog number: CLS431751)

3. 2 chambered coverslip bottom dishes (Lab-Tek, chambered coverglass, No. 1, Thermo, catalog number: 155380). Alternatively, any number 1 coverslip bottom chamber compatible with the microscope stage can be used, such as a coverslip bottom Petri dish.
4. 00 number paintbrush or fine paintbrush (Camlin, India, catalog number: 2052769)
5. *Drosophila* stocks- Sqh-mCherry expressing control (BDSC, catalog number: 59024) and $graf^{CR57}$ mutant flies generated in the RR lab.
6. Pasteur Pipette (Tarsons, India, catalogue number: 940050)
7. Yeast paste on sugar agar media in Petri plates (PRIME Instant Dry Yeast)
8. Deionized water
9. Embryo collection cages (59-100, Flystuff.com)
10. Sucrose (non-mol bio grade local purchase)
11. Agar-agar (non-mol bio grade local purchase)
12. 100% sodium hypochlorite-bleach (Sigma, catalog number: 1056142500)
13. Phosphate buffered saline (PBS)
14. Cornmeal agar *Drosophila* medium in vials
15. NaCl (non-mol bio grade local purchase)
16. KCl (non-mol bio grade local purchase)
17. Na_2HPO_4 (non-mol bio grade local purchase)
18. KH_2PO_4 (non-mol bio grade local purchase)
19. Malt (non-mol bio grade local purchase)
20. Cornflour (non-mol bio grade local purchase)
21. Propionic Acid (non-mol bio grade local purchase)
22. Orthophosphoric acid (non-mol bio grade local purchase)
23. Ethanol (non-mol bio grade local purchase)
24. PBS (10×) (see Recipes)
25. Fly media (see Recipes)
26. Sucrose-agar for embryo collection (see Recipes)

Equipment

1. Laser scanning confocal microscope, LSM 780 Zeiss confocal microscope (Zeiss, Jena, Germany) equipped with:
   a. Acoustic optical tunable filter (AOTF), for ablation of selected areas
   b. Femtosecond multiphoton pulsed Mai Tai laser (700–1,100 nm, ~2,000 mW power)
   c. 561 nm Diode laser (10mW laser power), for excitation of Sqh-mCherry
   d. Bandpass filter at 610 nm, for the emission of Sqh-mCherry fluorescence
   e. 40× objective, 1.4 NA Plan Apochromat (Zeiss) oil immersion lens
   f. Dichroic and emission filters, for the use of the 561 nm laser lines and detection of mCherry fluorescence
2. *Drosophila* Incubator at 25°C (Panasonic)
3. Stereo microscope 10× magnification (Olympus SZX10)

Software

1. ImageJ/Fiji (Schindelin *et al*., 2012) (https://imagej.net/software/fiji/downloads)
2. ImageJ/Fiji plugin- Bio-formats plugin (https://imagej.net/formats/bio-formats)
3. ImageJ/Fiji plugin, Manual_Tracking.java (https://imagej.nih.gov/ij/plugins/track/track.html)
4. Microsoft Excel (https://www.microsoft.com/en-in/microsoft-365/excel)
5. GraphPad Prism (https://www.graphpad.com/scientific-software/prism/)

Procedure

A. Embryo sample preparation

1. Maintain control Sqh-mCherry and *Graf*^{ER57}; Sqh-mCherry flies at 25°C, on standard cornmeal agar *Drosophila* medium in the vials.
2. Add 3-day old mated Sqh-mCherry and *Graf*^{ER57}; Sqh-mCherry males and females to fly collection cages containing 3% sucrose-agar plates supplemented with freshly made yeast paste. Allow them to get acclimatized to the cage for at least two days. Replace the plate with a fresh yeast paste each day.
3. Add a fresh plate containing yeast paste and collect embryos for 30 min. Discard this collection because it will contain embryos of older ages. Add a fresh plate and collect embryos for 2.5 h. The maximum age of the embryos in this collection will be 2.5 h.
4. Add water to the embryo collection plates. Use a fine brush to gently dislodge the embryos from the agar in water, and pour them into a cell strainer (Figure 1A). Wash the embryos with water until the yeast paste is thoroughly washed off, and transfer the remaining embryos into the cell strainer. Immerse the cell strainer containing embryos in 100% sodium hypochlorite for 1 min in a slightly larger plate, to remove the embryonic chorion (Figure 1B).
5. Wash dechorionated embryos three times with water to remove any residual bleach.
6. Once embryos are washed, then the cell strainer containing embryos is placed on a fresh plate containing some water, to keep embryos hydrated.
7. Using a fine brush, move individual dechorionated embryos carefully, removing excess water by drying the brush on tissue paper. Align the embryos in one of the wells of a 2-chambered coverglass bottom dish under visualization by a 10× objective in a stereomicroscope. Apply gentle pressure with the brush, to place the embryos such that the largest surface area comes in contact with the coverslip. Approximately 20 embryos can be placed in a line in each well of the 2-chambered coverglass dish (Figure 1C). Ensure that the embryos are evenly spaced apart from each other. The orientation of the embryo does not matter for the cellularization stage. The embryo needs to be oriented on the ventral side towards the coverglass, if experiments are planned during gastrulation.
8. Using a Pasteur pipette, carefully add 2 mL of 1× PBS to immerse the embryos.
9. Add oil to the 40×/1.4NA objective in the Zeiss LSM780 confocal microscope (Figure 1C). Place the coverslip bottom chambers containing embryos on the microscope stage to perform ablations.

Notes:

1. *This protocol employs embryos containing a fluorescently tagged light chain of Myosin II, Sqh, Sqh-mCherry for ablations. Sqh-mCherry labels the contractile ring throughout cellularization. Care should be taken to ensure that the marker used for laser ablation is recruited to the structure where laser ablation is planned, and does not itself change the contractile properties of the structure.*
2. *Decide the magnification of the objective lens available in the microscope for imaging based on the tissue of interest.*

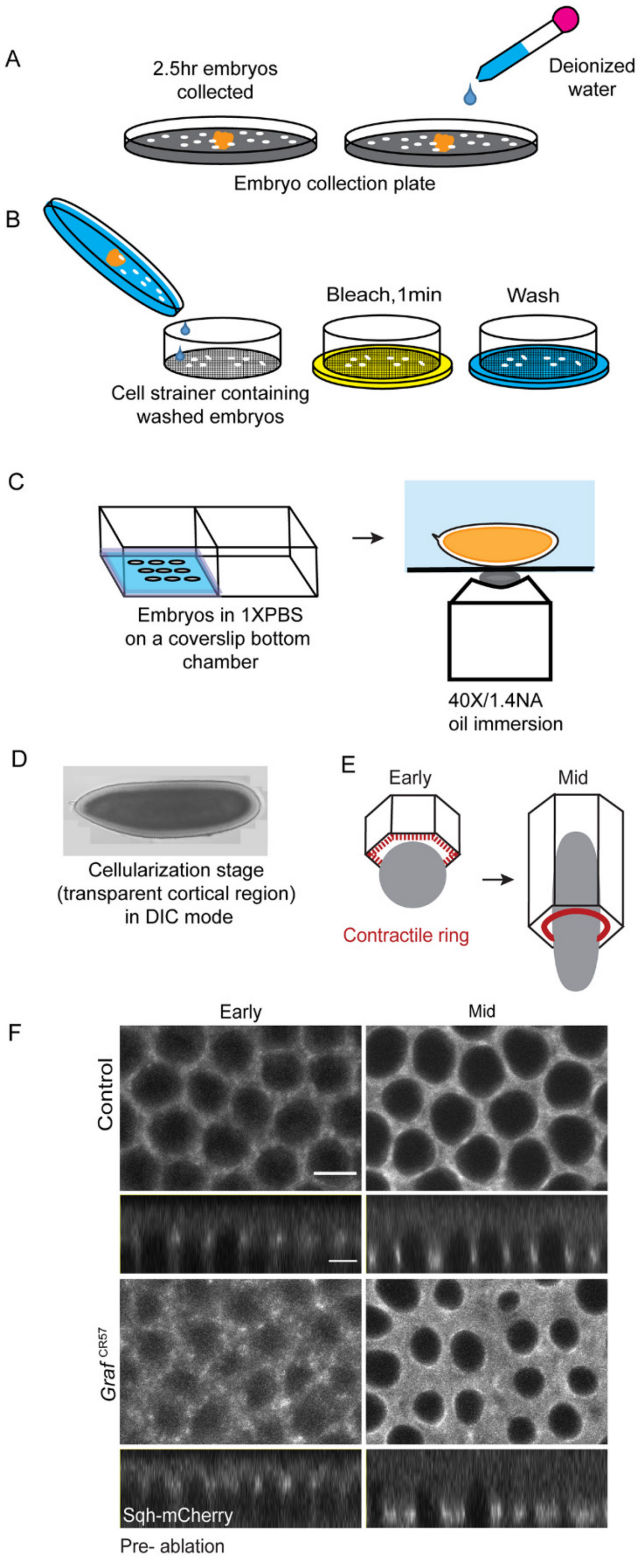

Figure 1. Live imaging of Sqh-mCherry expressing embryos.

(A–C) Schematic showing the procedure for embryo collection. Flies expressing Sqh-mCherry are added to the fly cage containing sucrose-agar plates with yeast paste. Embryos are collected for 2.5 h and then gently washed in water using a brush without damaging the embryos (A). Washed embryos are collected in a cell strainer and

placed in a plate containing 100% sodium hypochlorite solution for 1 min, to remove the chorion membrane (B). Embryos are washed thoroughly with water three times to ensure removal of residual bleach. Individual dechorionated embryos are picked with a brush and placed on a coverslip bottom chamber. The embryos are oriented such that the maximum surface area comes in contact with the coverglass. Embryos are mounted ensuring appropriate spacing between them in a coverslip bottom chamber, and are covered with 2 mL of PBS. The chamber is placed in the microscope stage on a 40×/1.4NA oil immersion objective. (D) A DIC image of the *Drosophila* embryo in cellularization shows the presence of a lighter semi-transparent cortical region. (E) Schematic showing the formation of the contractile ring in cellularization. Sqh-mCherry marks the tip of the furrow (red). In the early stages of cellularization, when the furrow length is below 6 µm, Sqh-mCherry is present in a patchy organization at the tip. In the mid-stages, when the furrow length is 6–15 µm, Sqh-mCherry is more uniformly present at the circular ring. (F) Sqh-mCherry distribution to mark the early and mid-stages for laser ablation. Grazing and sagittal optical sections from control and *Graf*^{CR57} mutant embryos expressing Sqh-mCherry at the furrow tip. The grazing section illustrates the distribution of Sqh-mCherry, and the sagittal view shows its localization at the furrow tip and the length of the furrow during cellularization. A z-stack is acquired and saved before proceeding to the laser ablation experiments. This z-stack image set is used to extract the sagittal views for the measurement of furrow length. Scale bar: 5 µm.

B. Image acquisition

1. Identify embryos in cellularization by visualizing them in DIC mode (Figure 1D). Embryos in cellularization have a transparent cortical region.
2. The actomyosin assembly leading to contractile ring formation and constriction occurs at the base of the extending furrow during cellularization. Actomyosin assembly takes place in the early stages, when the furrow length of below 6 µm. Actomyosin ring constriction occurs in the mid-stages of cellularization, when the furrow length is 6–15 µm (Figure 1E, F).
3. Observe the embryos in DIC or bright field mode using the 40×/1.4NA objective, to identify the stage of development of embryos. Cellularization is identified by the presence of a transparent cortical region. The early and mid-stages of cellularization can be distinguished by the furrow length in the bright field, or by the Sqh-mCherry fluorescence (Figure 1F).
4. Focus a region of interest in cellularizing embryos at the furrow tip. Sqh-mCherry fluorescence is visible using 561 nm excitation at 2% laser power. Acquire images at 5× optical zoom and 512 × 512 pixels, with 2-averaging and 0.7 µm-thick optical sections. Before ablation, take a z-stack of the embryo, from apical sections up to the bottom of the furrow tip, to measure furrow length in orthogonal views.
5. Select the time-lapse and photobleaching programs on the software.
6. Select the region of interest (ROI) by focusing the embryo at zoom 5. Select a line across the image with dimensions of 42.5 µm (512 pixels) with width zero. The ROI size covers approximately 10 rings in the selected frame (Figure 2A).
7. Select the 800 nm laser line on the Mai-Tai laser and adjust the laser power to 25–30%, with 20 iterations. The actual time taken for laser ablation with these settings and ROI dimensions was 2.699s.
8. Select the settings in the software: acquire three images before the ablation, and 60 images after ablation, with a 0-time interval in the time series mode, using the 561 nm laser for excitation at 2% power (Figure 2B, C).
9. Start the experiments and save the pre-ablated and ablated movie files separately.
10. Save the image with the information of the line used for ablation (Video 1).

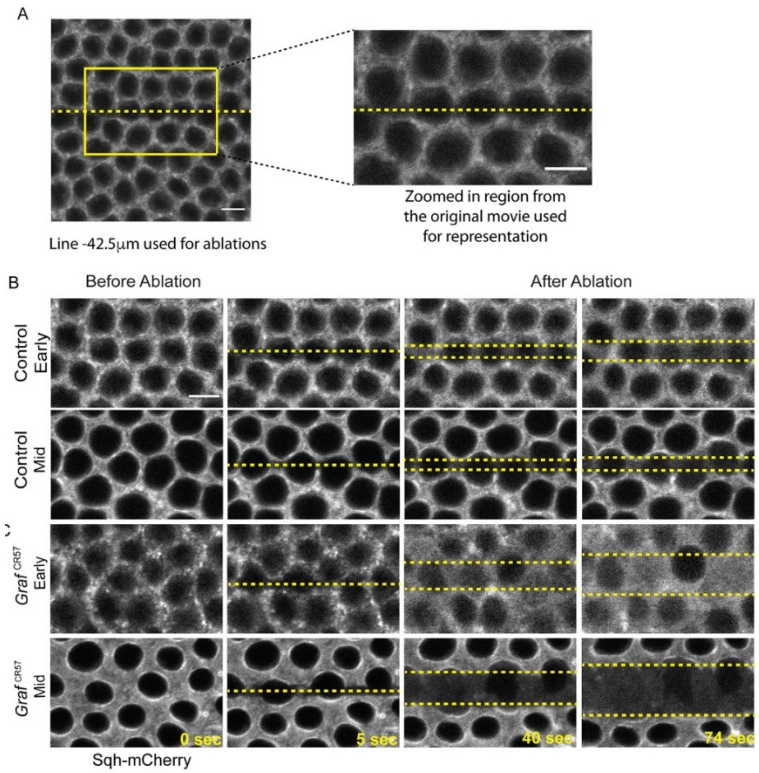

Figure 2. Optical sections showing laser ablations in control and *Graf*^{CR57} embryos expressing Sqh-mCherry.

(A) An optical section from the movie shows a 42.51 µm line used for ablations, and a zoomed in region used for further representation. (B) The region of interest in embryos is scanned three times before ablations. During ablations, a 42.51 µm line is drawn to mark the region for ablation (yellow dotted line). The ablation takes 2.699s. Imaging is carried out at a speed of 1.58 µs per pixel. Laser ablations are carried out with 20 iterations, using the 800 nm multiphoton laser with 25–30% laser power. Imaging is carried out for approximately 80 sec. The ablated regions move away from each other (yellow dotted lines) (Video 1). (C) *Graf*^{CR57} embryos show constricted rings during cellularization, along with increased movement of the ablated edges, when compared to controls (Video 1). Scale bar: 5 µm

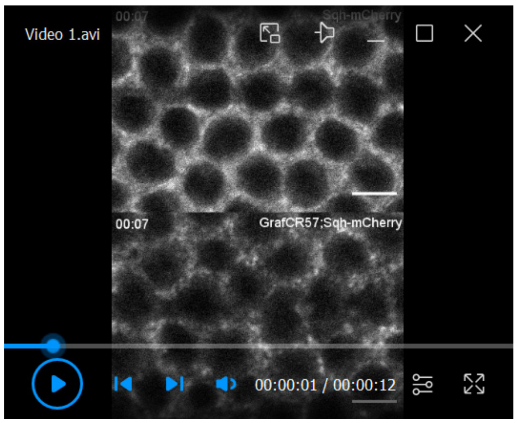

Video 1. Laser ablation movie.

Control Sqh-mCherry and *Graf*^{CR57}; Sqh-mCherry embryos were subjected to laser ablation in the optical section at the furrow tip (marked in yellow line) in early cellularization. Time is in sec. Scale bar: 5 µm

Notes:

1. *The parameters of laser power at 800 nm, iterations, depth, ROI size, and acquisition timings are crucial for obtaining successful laser ablations within the tissue.*
2. *Optimizing the laser power at 800 nm and iterations is an important step for standardizing the conditions for laser ablation. At very high laser powers, the vitelline and plasma membranes will rupture, causing a leak of cytoplasmic contents in the regions of the embryo designated for laser ablation. In addition, high laser power may result in tissue cauterization (Rauzi et al., 2015). During the initial steps, high laser power showing damage confirms the technical functionality of the laser. At very low laser powers, photobleaching followed by fluorescence recovery will occur, and no ablation will occur. An optimal laser power should be used such that ablation takes place, and the edges are seen to drift away from each other after the ablation.*
3. *We have used a femtosecond pulsed laser with 800 nm wavelength. A range of infrared wavelengths have been used for laser ablation ranging from 800 to 1030 nm in Drosophila embryo cells (Rauzi et al., 2008, 2015; Krueger et al., 2019; Sharma and Rikhy, 2021). The penetration depth is likely to affect the efficiency of laser ablation, however, a range of infrared wavelengths approximately 800–950 nm have been found to be equally suitable for ablation in Drosophila embryos (Supatto et al., 2005).*
4. *ROI size and shape optimization is required, based on the cell structure targeted for ablations. A line ROI across several rings in the 42.51 µm in this study is used in cellularization, to cause a significant displacement to permit calculation of recoil velocity with reproducibility.*
5. *The laser power needed for ablation may change at different depths of the furrow tip where the contractile ring assembles during cellularization. The displacement should be compared between movies for laser ablation performed at approximately the same depth of furrows in cellularization for controls and mutants. The ring architecture, as well as composition and viscosity of the medium are likely to change with different depths in cellularization.*
6. *Relaxation of the ring after ablation is specific to the furrow tip containing the actomyosin distribution. The relaxation obtained in the polygonal junctional regions in apical sections above the furrow tip is almost negligible. This lack of displacement of edges in the junctional regions also highlights the function of actomyosin for increasing contractility in the ring at the furrow tip.*
7. *Adjust the total time of acquisition after ablation based on the process being studied. In the present case, the imaging was carried out for 60 cycles for a total of approximately 75 s. The furrow tip will keep ingressing into the embryo as the imaging proceeds, due to embryo development. Hence, the furrow tip will move out of focus while imaging. If a greater time duration of imaging is desired for cellularization or in other stages of development, a z-stack along with a time series may be acquired, to obtain information about displacement in the ablated region. For most processes, imaging should be carried out until the displacement change saturates over time.*
8. *The movement of the ablated edge is relatively fast just after ablation, and slows down over time until saturation is achieved. It may not be possible to achieve saturation of displacement in the imaging settings for the experiment. It is important to run the control and mutant experiments simultaneously, to compare the difference in displacement between them.*

C. Image Processing

1. Open the acquired pre-ablated and ablated movies using ImageJ/Fiji software (https://imagej.net/formats/bio-formats).
2. Add the ROI used for ablation using the bio formats plugin. Alternatively, add the ROI manually by placing the image containing the ROI information in the movie file in Fiji.
3. Select the orthogonal view from the stacks tab in Fiji for the pre-ablated z-stack images. Select the line option to mark and measure the furrow length, to identify and segregate the early and mid-cellularization stages. Analyze the movies in groups in the early (less than 6 µm furrow length) and mid-stages (6–15 µm furrow length) of cellularization.
4. Adjust brightness and contrast using the “Auto” option for the ablated movies, to visualize the contractile ring edges for quantification.

D. Image analysis

1. Download the Manual_Tracking.java plugin from the Image J/Fiji plugins website at https://imagej.nih.gov/ij/plugins/track/track.html. Add this to the plugins folder and restart Image J/Fiji to find this in the Plugin tab. Open the manual tracking plugin of Fiji software from the tracking tab (Figure 3A).
2. Select the points on the edges of the ablated ring for the estimation of displacement. The edges away from the ablation site are suitable for the estimation of displacement in this experiment, because they remain brightly visible throughout the movie. The brightness and contrast tool may be used to adjust the fluorescence and identify the edges more distinctly.
3. The XY coordinates of these points appear in the results sheet in the plugin. Add new points in the successive images until the end of the time series, to track the displacement of the edge (Figure 3A).
4. The plugin will extract XY coordinates of the selected points in the results sheet (Figure 3A).
5. Export the XY coordinate values obtained from Fiji into Microsoft Excel for further calculations. The x1y1 coordinate marked the bottom edge and the x2y2 coordinate marked the edge above the ablated region (Figure 3B). The coordinates are extracted in pixels from the image.
6. Convert values of XY coordinates from pixel to µm values, dividing by the scaling factor of 12.0443. Place the XY values in µm under the bottom (x1y1) and top (x2y2) section in the excel sheet (Figure 3C).
7. Apply the equation below to extract displacement values for all time points from start to end of movies from controls and mutants (Figure 4A).

$$D = \sqrt{(y2 - y1)^2 + (x2 - x1)^2}$$

where D = displacement
x1 and y1 = coordinates of edge below the ablated region
x2 and y2 = coordinates of edge above the ablated region

8. Subtract the distance obtained for the coordinates before ablations (Figure 4B, values marked in green) from the subsequent time points at or after the ablations (values marked in red).
9. Mark the first time point after laser ablation as time point 0 (highlighted in yellow in Figure 4B).
10. Calculate the displacement similarly from five embryos per genotype (Figure 4C) and plot a displacement versus time graph in GraphPad Prism (Figure 4D).
11. The displacement versus time graph for each embryo is further used for extracting maximum displacement and recoil velocity (Figure 5A).
12. The displacement at the final time point of approximately 75 s is used to extract the maximum displacement from each embryo (Figure 5B).
13. Use the first 20 data points from the displacement vs time graph to extract the recoil velocity from each embryo (Figure 5C). Fit these data points to a linear function using the linear equation y = mx + c. The slope m from the linear equation is the recoil velocity. Plot the recoil velocity from individual control and *Graf*^{ICR57} mutant embryos using GraphPad Prism (Figure 5D).

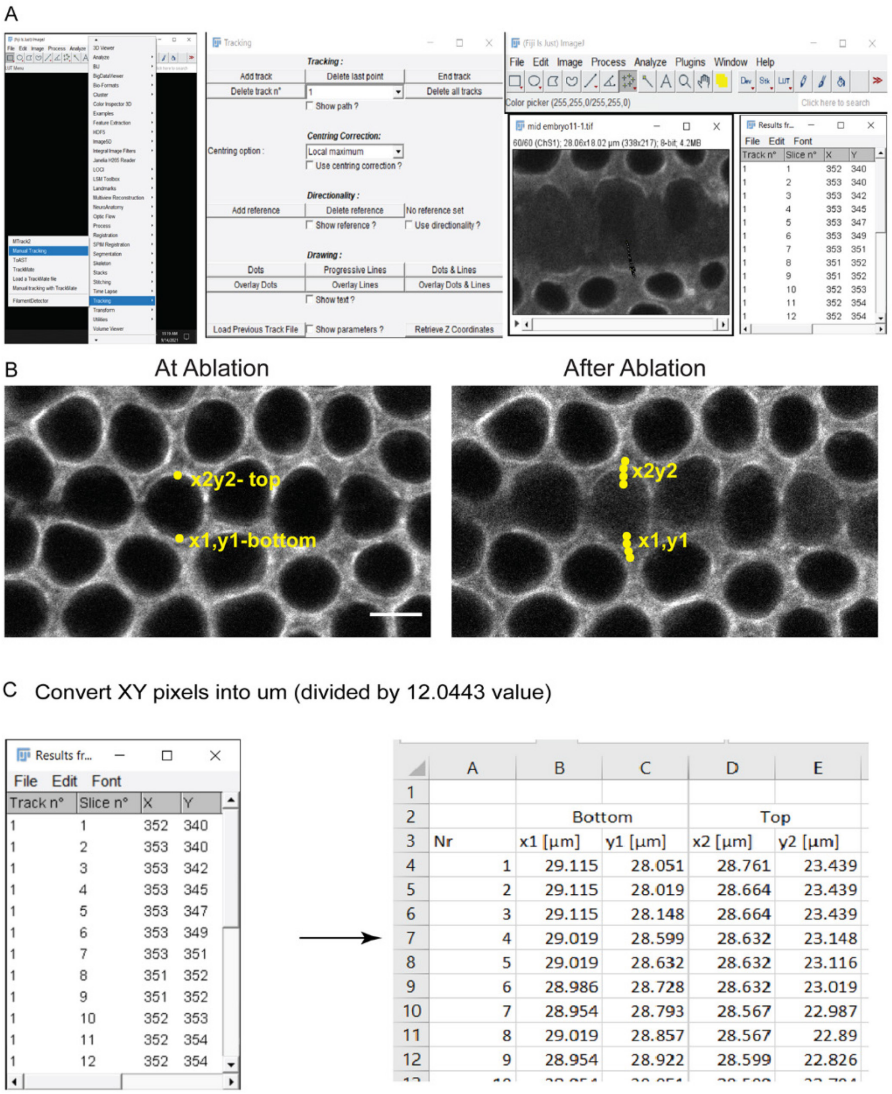

Figure 3. Extracting XY coordinates from ablated edges.
(A) Open the laser ablation movies in Image J/Fiji. Open the Manual tracking plugin from the Tracking tools. Select the "add track" tab and click on a specific point near ablations to score for the movement of the edge. The results window provides XY coordinates of selected points during ablations. The image shows points marked in subsequent sections as the edges move away from each other (yellow arrowhead). (B) Control embryos expressing Sqh-mCherry are shown with marks on the bottom edge as x1y1 and the top edge as x2y2 during and after ablations, respectively. (C) Convert the XY coordinates from pixels into µm by multiplying by the scaling factor (12 pixels/µm). Scale bar: 5 µm.

A Distance calculation using XY coordinates

$$D=\sqrt{(y2-y1)^2+(x2-x1)^2}$$

D= distance
x2,x1 & y2,y1 are xy coordinates

B

	A	B	C	D	E	F	G	H	I
1	embryo9								
2									
3	S.No	Actual time (sec)	Time (sec) alloted after ablations	Bottom		Top		Distance	Displacement
4				x1 [µm]	y1 [µm]	x2 [µm]	y2 [µm]	= SQRT((y2-y1)^2+(x2-x1)^2)	= ($D_{ablated}$ - $D_{pre-ablated}$)
5	1	0		29.115	28.051	28.761	23.439	4.626	
6	2	1.253		29.115	28.019	28.664	23.439	4.602	
7	3	2.501		29.115	28.148	28.664	23.439	4.731	
8	4	5.2	0	29.019	28.599	28.632	23.148	5.465	0.734
9	5	6.244	1.04	29.019	28.632	28.632	23.116	5.530	0.799
10	6	7.49	2.29	28.986	28.728	28.632	23.019	5.720	0.989
11	7	8.742	3.54	28.954	28.793	28.567	22.987	5.819	1.088
12	8	9.993	4.79	29.019	28.857	28.567	22.89	5.984	1.254
13	9	11.232	6	28.954	28.922	28.599	22.826	6.106	1.376
14	10	12.482	7.3	28.954	29.051	28.599	22.794	6.267	1.537
15	11	13.732	8.5	28.954	29.019	28.599	22.729	6.300	1.569
16	12	14.983	9.8	28.954	29.083	28.599	22.729	6.364	1.633

C

		X	Group A	Group B	Group C	Group D	Group E	Grou
		Time(sec)	embryo1	embryo2	embryo3	embryo4	embryo5	Tit
		X	Y	Y	Y	Y	Y	Y
1	Title	0.00	0.734172	0.450941	0.160608	0.158192	0.320520	
2	Title	1.04	0.799011	0.551792	0.194813	0.285782	0.513473	
3	Title	2.29	0.989417	0.646349	0.323465	0.322071	0.674419	
4	Title	3.54	1.088335	0.742309	0.355381	0.248556	0.580893	
5	Title	4.79	1.253547	0.874489	0.457038	0.442918	0.613860	
6	Title	6.00	1.375780	0.939910	0.415971	0.570235	0.709765	
7	Title	7.30	1.536515	1.033168	0.511805	0.602205	0.773703	
8	Title	8.50	1.569462	1.066149	0.545697	0.670272	0.805387	
9	Title	9.80	1.633361	1.163096	0.514761	0.744814	0.935555	
10	Title	11.00	1.762164	1.258117	0.578631	0.727836	1.031238	
11	Title	12.30	1.890975	1.229592	0.708517	0.852796	1.034550	

D

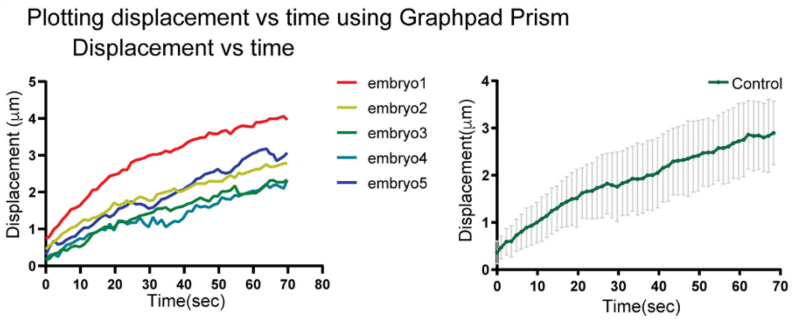

Figure 4. Extracting and plotting displacement versus time graph from XY coordinates.
(A) Displacement is extracted using the formula shown; X and Y represent the coordinates obtained in Figure 3. (B) Displacement of edges in pre-ablated sections (values in green) is subtracted from the displacement at

the ablated time point (values in red). The row highlighted in yellow is the first time point after the ablation, this is marked as the time point 0. (C) Data points showing displacement with respect to time from five embryos are plotted with Graphpad Prism. (D) Individual plots of displacement with respect to time are shown. The average ± SEM plot from 5 embryos is plotted using GraphPad Prism.

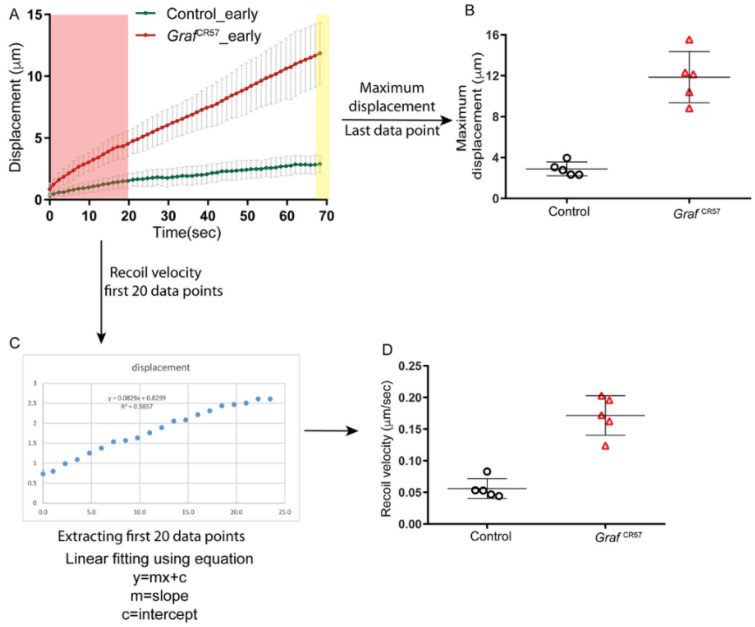

Figure 5. Quantifying maximum displacement and recoil velocity from the displacement versus time graph.

(A) Displacement versus time graph for control and *Graf*^{CR57} is used for extracting maximum displacement (marked in yellow) and recoil velocity (from the region marked in light red). (B) The maximum displacement is plotted by extracting the last data point from the displacement versus time graph. (C) The first 20 data points are used for quantifying recoil velocity from displacement versus time graph. The plot is fit to a linear equation, and the slope is extracted from the linear equation. (D) The slope of each line gives the recoil velocity, which is plotted using GraphPad Prism. *Graf*^{CR57} embryos show significantly increased maximum displacement and recoil velocity when compared to control embryos during early cellularization.

Notes:

1. *If the stage of development where ablations are being performed has significant intrinsic movement, then obtain the extent of displacement in these stages from a movie of the same duration before ablations are performed. This intrinsic displacement can be subtracted from all the coordinates obtained after laser ablation.*
2. *Recoil velocity is the fastest close to the ablation time point. The time points after the ablation used to calculate the recoil velocity should be such that the slope can be extracted reproducibly from this time window. The variability may increase if recoil velocity calculations are attempted from fewer than 20 time points in Figure 5.*
3. *Viscosity and tension influence the recoil velocity. There are inherent differences in viscosity at different depths of embryos during cellularization (Wessel et al., 2015). We control for the viscosity at different depths by performing ablations at approximately similar furrow lengths in the control and mutant embryos.*

Recipes

1. **PBS (10×)**
   NaCl: 1.37 M
   KCl: 27 mM
   Na_2HPO_4: 100 mM
   KH_2PO_4: 18 mM

   Note: Prepare and store 10× PBS at 4°C for long-term usage. Prepare fresh 1× PBS by diluting the 10× PBS stock solution with autoclaved distilled water.

2. **Fly media**

   Note: The amount of ingredients is mentioned per liter.

   Agar: 10 g
   Yeast: 15 g
   Malt: 30 g
   Cornflour: 75 g
   Sugar: 80 g
   Water: 900 mL
   Propionic Acid: 5 mL
   Orthophosphoric acid: 1 mL
   Alcohol: 5 mL
   5% methyl para hydroxybenzoate (in alcohol): 0.25 g in 5 mL of alcohol

3. **Sucrose-agar for embryo collection**
   Sucrose: 3%
   Agar: 2.5%
   Add sucrose and agar to autoclaved deionized water and boil in a microwave oven till the agar dissolves uniformly. Pour this medium into the 60 mm Petri dish and let it cool at room temperature. Cover these plates with lids and store them at 4°C after the medium solidifies.

Acknowledgments

We thank the *Drosophila* facility at IISER Pune for help with maintaining fly stocks. We thank the IISER Pune microscopy facility for help with imaging during the experiment. Stocks from Bloomington *Drosophila* Stock Center, Indiana, USA were used in this study. The lab is supported by funding from IISER Pune, India, Department of Biotechnology, India and Department of Science and Technology, India. SS is supported by a graduate fellowship from the Council of Scientific and Industrial Research, India. This protocol has been verified in Sharma and Rikhy (2021), eLife, doi: 10.7554/eLife.63535.

Competing interests

The authors declare no competing interests.

References

Carim, S. C., Kechad, A. and Hickson, G. R. X. (2020). Animal Cell Cytokinesis: The Rho-Dependent Actomyosin-Anilloseptin Contractile Ring as a Membrane Microdomain Gathering, Compressing, and Sorting Machine. *Front Cell Dev Biol* 8: 575226.

Foe, V. E. and Alberts, B. M. (1983). Studies of nuclear and cytoplasmic behaviour during the five mitotic cycles that precede gastrulation in *Drosophila* embryogenesis. *J Cell Sci* 61: 31-70.

He, B., Martin, A. and Wieschaus, E. (2016). Flow-dependent myosin recruitment during *Drosophila* cellularization requires zygotic dunk activity. *Development* 143(13): 2417-2430.

Heer, N. C. and Martin, A. C. (2017). Tension, contraction and tissue morphogenesis. *Development* 144(23): 4249-4260.

Kong, D., Wolf, F. and Grosshans, J. (2017). Forces directing germ-band extension in *Drosophila* embryos. *Mech Dev* 144(Pt A): 11-22.

Krueger, D., Quinkler, T., Mortensen, S. A., Sachse, C. and De Renzis, S. (2019). Cross-linker-mediated regulation of actin network organization controls tissue morphogenesis. *J Cell Biol* 218(8): 2743-2761.

Liang, X., Michael, M. and Gomez, G. A. (2016). Measurement of Mechanical Tension at Cell-cell Junctions Using Two-photon Laser Ablation. *Bio-protocol* 6(24): e2068.

Paluch, E. and Heisenberg, C. P. (2009). Biology and physics of cell shape changes in development. *Curr Biol* 19(17): R790-799.

Priya, R. and Yap, A. S. (2015). Active tension: the role of cadherin adhesion and signaling in generating junctional contractility. *Curr Top Dev Biol* 112: 65-102.

Rauzi, M., Krzic, U., Saunders, T. E., Krajnc, M., Ziherl, P., Hufnagel, L. and Leptin, M. (2015). Embryo-scale tissue mechanics during *Drosophila* gastrulation movements. *Nat Commun* 6: 8677.

Rauzi, M., Verant, P., Lecuit, T. and Lenne, P. F. (2008). Nature and anisotropy of cortical forces orienting *Drosophila* tissue morphogenesis. *Nat Cell Biol* 10(12): 1401-1410.

Schindelin, J., Arganda-Carreras, I., Frise, E., Kaynig, V., Longair, M., Pietzsch, T., Preibisch, S., Rueden, C., Saalfeld, S., Schmid, B., *et al*. (2012). Fiji: an open-source platform for biological-image analysis. *Nat Methods* 9(7): 676-682.

Sharma, S. and Rikhy, R. (2021). Spatiotemporal recruitment of RhoGTPase protein GRAF inhibits actomyosin ring constriction in *Drosophila* cellularization. *Elife* 10: e63535.

Supatto, W., Debarre, D., Moulia, B., Brouzes, E., Martin, J. L., Farge, E. and Beaurepaire, E. (2005). *In vivo* modulation of morphogenetic movements in *Drosophila* embryos with femtosecond laser pulses. *Proc Natl Acad Sci U S A* 102(4): 1047-1052.

Wessel, A. D., Gumalla, M., Grosshans, J. and Schmidt, C. F. (2015). The mechanical properties of early *Drosophila* embryos measured by high-speed video microrheology. *Biophys J* 108(8): 1899-1907.

Xue, Z. and Sokac, A. M. (2016). -Back-to-back mechanisms drive actomyosin ring closure during *Drosophila* embryo cleavage. *J Cell Biol* 215(3): 335-344.